

# Large Improvement in the Catalytic Activity Due to Small Changes in the Diimine Ligands: New Mechanistic Insight into the Dirhodium(II,II) Complex-Based Photocatalytic H<sub>2</sub> Production

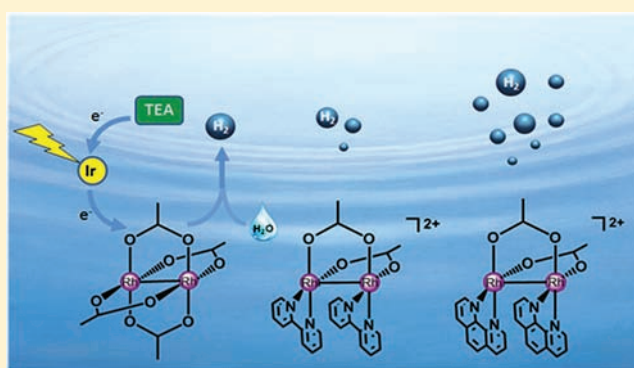
Jingfan Xie,<sup>†,‡</sup> Chao Li,<sup>†</sup> Qianxiong Zhou,<sup>†</sup> Weibo Wang,<sup>†</sup> Yuanjun Hou,<sup>\*,†</sup> Baowen Zhang,<sup>†</sup> and Xuesong Wang<sup>\*,†</sup>

<sup>†</sup>Key Laboratory of Photochemical Conversion and Optoelectronic Materials, Technical Institute of Physics and Chemistry, Chinese Academy of Sciences, Beijing 100190, People's Republic of China

<sup>‡</sup>Graduate School of Chinese Academy of Sciences, Beijing 100049, People's Republic of China

## S Supporting Information

**ABSTRACT:** Two dirhodium(II) complexes, [Rh<sup>II</sup><sub>2</sub>(μ-O<sub>2</sub>CCH<sub>3</sub>)<sub>2</sub>(bpy)<sub>2</sub>](O<sub>2</sub>CCH<sub>3</sub>)<sub>2</sub> (Rh<sub>2</sub>bpy<sub>2</sub>; bpy = 2,2'-bipyridine) and [Rh<sup>II</sup><sub>2</sub>(μ-O<sub>2</sub>CCH<sub>3</sub>)<sub>2</sub>(phen)<sub>2</sub>](O<sub>2</sub>CCH<sub>3</sub>)<sub>2</sub> (Rh<sub>2</sub>phen<sub>2</sub>; phen = 1,10-phenanthroline) were synthesized, and their photocatalytic H<sub>2</sub> production activities were studied in multicomponent systems, containing [Ir<sup>III</sup>(ppy)<sub>2</sub>(dtbbpy)]<sup>+</sup> (ppy = 2-phenylpyridine, dtbbpy = 4,4'-di-*tert*-butyl-2,2'-bipyridine) as the photosensitizer (PS) and triethylamine as the sacrificial reductant (SR). There is a more than 6-fold increase in the photocatalytic activity from Rh<sub>2</sub>bpy<sub>2</sub> to Rh<sub>2</sub>phen<sub>2</sub> just using phen in place of bpy. A turnover number as high as 2622 was obtained after 50 h of irradiation of a system containing 16.7 μM Rh<sub>2</sub>phen<sub>2</sub>, 50 μM PS, and 0.6 M SR. The electrochemical, luminescence quenching, and transient absorption experiments demonstrate that Rh<sup>I</sup>Rh<sup>I</sup> is the true catalyst for the proton reduction. The real-time absorption spectra confirm that a new Rh-based species formed upon irradiation of the Rh<sub>2</sub>phen<sub>2</sub>-based multicomponent system, which exhibits an absorption centered at ~575 nm. This 575-nm intermediate may account for the much higher H<sub>2</sub> evolution efficiency of Rh<sub>2</sub>phen<sub>2</sub>. Our work highlights the importance of N-based chelate ligands and opens a new avenue for pursuing more efficient Rh<sup>II</sup><sub>2</sub>-based complexes in photocatalytic H<sub>2</sub> production application.



## INTRODUCTION

The conversion of solar energy into clean chemical fuel, such as H<sub>2</sub> production by photolysis of water, is considered to be one of the feasible ways to solve the energy crisis.<sup>1–3</sup> To achieve the ultimate goal of the overall water splitting, many efforts have been paid to optimize H<sub>2</sub> and O<sub>2</sub> evolution half-reactions separately.<sup>4–8</sup> For the reductive side of the water splitting, the multicomponent system, involving a photosensitizer (PS) to harvest sun light, a water reduction catalyst (WRC) to overcome the activation energy for H<sub>2</sub> production, an electron relay (ER) to facilitate electron transfer from PS to WRC, and a sacrificial reductant (SR) to recycle PS, has been extensively and intensively studied for more than 3 decades.<sup>9,10</sup> Recently, a variety of combinations of molecular PS and WRC showed high H<sub>2</sub> production efficiencies.<sup>11–18</sup> While the molecular PSs utilized include organic dyes and transition-metal complexes, the molecular WRCs explored so far are exclusively transition-metal complexes, and Pt,<sup>6,16b</sup> Pd,<sup>16a</sup> Rh,<sup>9,10,18</sup> Fe,<sup>13</sup> Ni,<sup>14</sup> and Co<sup>8,11,12,15,17</sup> predominate the central metals of these complexes. Of them, rhodium complexes, e.g., [Rh<sup>III</sup>(bpy)<sub>3</sub>]<sup>3+</sup> (bpy = 2,2'-bipyridine), represent the earliest studied molecular

WRCs.<sup>19</sup> Also, rhodium complexes are among the most efficient molecular WRCs. By the proper combination of [Rh<sup>III</sup>(dtbbpy)<sub>3</sub>]<sup>3+</sup> (dtbbpy = 4,4'-di-*tert*-butyl-2,2'-bipyridine) with an Ir<sup>III</sup>-based PS and careful optimization of the reaction conditions, Bernhard and co-workers developed a multicomponent water reduction system that achieves a turnover number (TON) of over 5000 (22 h of irradiation).<sup>18</sup> Rh is also utilized as a WRC in a single-component system in which PS, ER, and WRC are delicately integrated into one molecule.<sup>20,21</sup> Brewer and co-workers recently reported a Ru–Rh–Ru single-component system, showing an unusually high TON (1300 mol of H<sub>2</sub> (mol of Rh)<sup>-1</sup> with long-term photolysis).<sup>21c</sup> Though Rh is in the catalogue of rare noble metals, it is still appealing to develop highly active and stable Rh-based WRCs to compensate for its weakness in cost.

Dinuclear rhodium complexes with the structural character of a Rh–Rh bond are extremely unique in photoinduced H<sub>2</sub> production. As early as 1977, Gray and co-workers found that

Received: March 29, 2012

Published: May 16, 2012

visible irradiation of an aqueous HCl solution containing  $[\text{Rh}^{\text{I}}(\mu\text{-BL})_4]^{2+}$  (BL = 1,3-diisocyanopropane) led to 1 equiv of  $\text{H}_2$ .<sup>22</sup> Nocera and Heyduk then developed a true photocatalytic  $\text{H}_2$  production system, in which photolysis of a mixed-valence dirhodium complex,  $[\text{Rh}^{\text{0II}}_2(\text{dfpma})_3\text{X}_2(\text{PPh}_3)]$  [dfpma = bis(difluorophosphino)methylamine, X = Cl or Br], led to 27 equiv of  $\text{H}_2$  during the initial 3 h of irradiation in the presence of 0.1 M HCl.<sup>23</sup> Recently, Sakai and co-workers realized  $\text{H}_2$  production photocatalyzed by a series of  $\text{Rh}^{\text{I}}\text{-Rh}^{\text{II}}$  complexes in a multicomponent system in aqueous acetate buffer (pH = 5).<sup>24</sup> The molecular PS, ER, and SR in the multicomponent system are  $\text{Ru}(\text{bpy})_3^{2+}$ , methylviologen ( $\text{MV}^{2+}$ ), and ethylenediaminetetraacetic acid disodium salt, respectively. Compared to Nocera's compound, Sakai's multicomponent system separates light harvesting from water reduction, more convenient for property optimization. Moreover, the photoreaction was carried out in an aqueous medium and a high concentration of acid is no longer needed. However, the TON value is not high, only 4.5 after 6 h of irradiation for  $[\text{Rh}^{\text{II}}_2(\mu\text{-O}_2\text{CCH}_3)_4(\text{H}_2\text{O})_2]$ . Only four dirhodium(II) complexes have been examined as WRCs so far. There may be large potential for such types of complexes to improve the catalytic activity, considering the fact that the bimetallic complexes that exhibit strong metal-metal interactions often afford new properties that are not available in mononuclear complexes.

In this work, two dirhodium(II) complexes,  $[\text{Rh}^{\text{II}}_2(\mu\text{-O}_2\text{CCH}_3)_2(\text{bpy})_2](\text{O}_2\text{CCH}_3)_2$  ( $\text{Rh}_2\text{bpy}_2$ ) and  $[\text{Rh}^{\text{II}}_2(\mu\text{-O}_2\text{CCH}_3)_2(\text{phen})_2](\text{O}_2\text{CCH}_3)_2$  ( $\text{Rh}_2\text{phen}_2$ ; phen = 1,10-phenanthroline), as shown in Scheme 1, were compared in detail as WRCs in a multicomponent system, where  $[\text{Ir}(\text{ppy})_2(\text{dtbbpy})]$  (ppy = 2-phenylpyridine; dtbbpy = 4,4'-di-*tert*-butyl-2,2'-bipyridine) acts as a PS and triethylamine (TEA) as a SR. While  $\text{MV}^{2+}$  was a necessary component for Sakai's system, no ER was used in our cases, demonstrating the interesting role

of the combination of PS and WRC. More importantly, the results reveal that a small structural change of the diimine ligand is possible to generate a significant effect on the water reduction activity, warranting further structure-activity studies of such kinds of Rh-based complexes.

## EXPERIMENTAL SECTION

**General Procedures.**  $\text{RhCl}_3 \cdot 3\text{H}_2\text{O}$  was purchased from Jilung Chemical Shanghai and was used as received. 1,10-Phenanthroline (phen) and 2,2'-bipyridine (bpy) were purchased from Alfa Aesar. Complexes  $[\text{Ir}(\text{ppy})_2(\text{dtbbpy})][\text{PF}_6]$  ( $[\text{Ir}]$ ),<sup>25</sup>  $\text{Rh}_2(\mu\text{-O}_2\text{CCH}_3)_4$ ,  $[\text{Rh}_2(\text{OAc})_4]$ ,  $[\text{Rh}_2(\mu\text{-O}_2\text{CCH}_3)_2(\text{phen})_2](\text{O}_2\text{CCH}_3)_2$  ( $\text{Rh}_2\text{phen}_2$ ), and  $[\text{Rh}_2(\mu\text{-O}_2\text{CCH}_3)_2(\text{bpy})_2](\text{O}_2\text{CCH}_3)_2$  ( $\text{Rh}_2\text{bpy}_2$ )<sup>26-28</sup> were prepared with literature methods. Triethylamine (TEA) and tetrahydrofuran (THF) were distilled prior to use. All other solvents were of analytical purity and were used without further treatment. Distilled water was used in all experiments.

<sup>1</sup>H NMR spectra were obtained on a Bruker DMX-400 MHz spectrophotometer. The mass spectrometry (MS) spectra were determined on a Q-ToF mass spectrometer (Waters). UV-vis absorption spectra were recorded on a Shimadzu UV-1601 spectrophotometer.

$[\text{Ir}(\text{ppy})_2(\text{dtbbpy})][\text{PF}_6]$ . <sup>1</sup>H NMR (400 MHz, acetone-*d*<sub>6</sub>):  $\delta$  8.87 (s, 2H), 8.23 (d, *J* = 8.1 Hz, 2H), 7.96 (dd, *J* = 16.6 and 6.3 Hz, 4H), 7.89 (d, *J* = 7.6 Hz, 2H), 7.78 (d, *J* = 5.4 Hz, 2H), 7.70 (dd, *J* = 5.9 and 1.9 Hz, 2H), 7.12 (t, *J* = 6.7 Hz, 2H), 7.02 (t, *J* = 7.5 Hz, 2H), 6.90 (t, *J* = 6.9 Hz, 2H), 6.33 (d, *J* = 6.9 Hz, 2H), 1.38 (d, *J* = 16.1 Hz, 18H). ESI-MS: *m/z* 768.5 ( $[\text{Ir}(\text{ppy})_2(\text{dtbbpy})]^+$ ).

$[\text{Rh}_2(\text{bpy})_2(\mu\text{-O}_2\text{CCH}_3)_2](\text{O}_2\text{CCH}_3)_2$ . <sup>1</sup>H NMR (400 MHz, MeOD):  $\delta$  8.34 (d, *J* = 5.5 Hz, 4H), 7.94 (dt, *J* = 15.4 and 6.9 Hz, 8H), 7.43-7.37 (m, 4H), 2.56 (s, 6H), 1.88 (s, 6H). ESI-MS: *m/z* 318.1 ( $[\text{Rh}_2(\text{bpy})_2(\mu\text{-O}_2\text{CCH}_3)_2]^{2+}$ ).

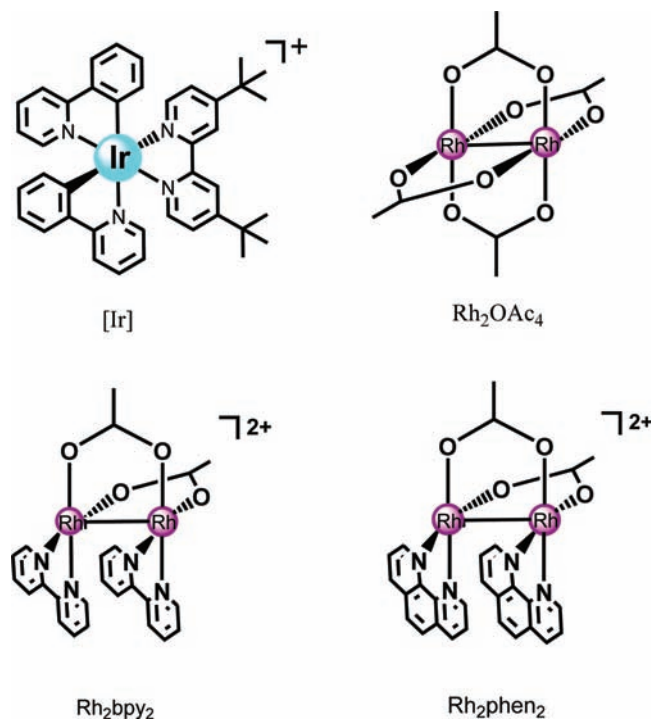
$[\text{Rh}_2(\text{phen})_2(\mu\text{-O}_2\text{CCH}_3)_2](\text{O}_2\text{CCH}_3)_2$ . <sup>1</sup>H NMR (400 MHz, MeOD):  $\delta$  8.56 (d, *J* = 5.2 Hz, 4H), 8.28 (d, *J* = 8.2 Hz, 4H), 7.71 (s, 4H), 7.63 (dd, *J* = 8.2 and 5.3 Hz, 4H), 2.68 (s, 6H), 1.86 (s, 6H). ESI-MS: *m/z* 342.1 ( $[\text{Rh}_2(\text{phen})_2(\mu\text{-O}_2\text{CCH}_3)_2]^{2+}$ ).

**H<sub>2</sub> Evolution Studies.** A total of 10 mL of a water/THF (2:8, v/v) solution containing 0.05 mM  $[\text{Ir}(\text{ppy})_2(\text{dtbbpy})]^+$ , 0.05 mM  $\text{Rh}^{\text{II}}_2$ -based catalyst, and 0.6 M TEA (835  $\mu\text{L}$ ) was put into a 40 mL glass vial equipped with a rubber-septum-sealed outlet. After bubbling with argon for 25 min, 3 mL of methane was injected into the reaction vessel to serve as the internal standard for  $\text{H}_2$  quantification. Then the vial was irradiated with visible light, which was obtained from a 1000 W solar simulator (Oriol 91192) using both a 350-nm-long pass glass filter and a distilled water pool to cut off the UV and IR light. The production of  $\text{H}_2$  was monitored and quantified by gas chromatography on a Shimadzu GC-2014 (thermal conductivity detector, 5 Å molecular sieve, 30 m  $\times$  0.53 mm column, N<sub>2</sub> gas carrier).

**Electrochemistry.** The redox potentials were measured on an EG&G model 283 potentiostat/galvanostat in a three-electrode cell with a platinum-wire working electrode, a platinum-plate counter electrode, and a SCE (saturated calomel electrode) reference electrode. Cyclic voltammetry was conducted at a scan rate of 100 mV s<sup>-1</sup> in an argon-saturated anhydrous dimethyl sulfoxide (DMSO) solution containing 0.1 M tetra-*n*-butylammonium hexafluorophosphate (*n*-Bu<sub>4</sub>NPF<sub>6</sub>) as the supporting electrolyte.

**Transient Absorption.** Nanosecond transient absorption measurements were performed on a LP-920 laser flash photolysis setup (Edinburgh). Excitation at 420 nm with a power of 2.0 mJ pulse<sup>-1</sup> from a computer-controlled Nd:YAG laser/OPO system from Opotek (Vibrant 355 II) operating at 10 Hz was directed to the sample with an optical absorbance of 0.4 at the excitation wavelength. The laser and analyzing light beam passed perpendicularly through a 1 cm quartz cell. The complete time-resolved spectra were obtained using a gated CCD camera (Andor iSTAR); the kinetic traces were detected by a Tektronix TDS 3012B oscilloscope and a R928P photomultiplier and analyzed by Edinburgh analytical software (LP920). All samples used in the flash photolysis experiments were deaerated for 30 min with argon before measurements.

Scheme 1. Chemical Structures of the Ir<sup>III</sup>-Based PSs and Rh<sup>II</sup><sub>2</sub>-Based WRCs



## RESULTS AND DISCUSSION

**Photocatalytic H<sub>2</sub> Production.** The H<sub>2</sub>-evolving activities of the Rh<sup>II</sup>-based catalysts were evaluated based on the TON defined as the produced H<sub>2</sub> molecule per catalyst molecule. The multicomponent system was used in the H<sub>2</sub>-evolving experiments, in which [Ir(ppy)<sub>2</sub>(dtbbpy)]<sup>+</sup> serves as a PS, the dirhodium(II) complexes as WRCs, and TEA as a SR. As shown in Table 1, each of the three components is necessary

**Table 1. Selected Control Experiments of Rh<sub>2</sub>phen<sub>2</sub>-Based Multicomponent Systems**

	PS (mM) = [Ir]	WRC (mM) = Rh <sub>2</sub> phen <sub>2</sub>	SR (M) = TEA	10 mL solvent (8:2, v/v)	TON (20 h irradiation)
1	0.05	0.05	0.6	THF/water	379
2	0.05	0.05	0	THF/water	0
3	0.05	0	0.6	THF/water	0
4	0	0.05	0.6	THF/water	0
6	0.05	0.05	0.6 (TEOA)	THF/water	46
5	0.05	0.05	0.6	pure water	3.3
7	0.05	0.05	0.6	CH <sub>3</sub> CN/ water	188

for photocatalytic H<sub>2</sub> production. It is worth noting that no ER was used in our multicomponent system, quite different from Sakai's system, where MV<sup>2+</sup> is a necessary component. The presence of MV<sup>2+</sup> even diminished the H<sub>2</sub> evolution efficiencies of our systems. Such a result presumably stems from the different combinations of PSs and WRCs, suggesting that the simultaneous structure optimization of PS and WRC is of importance to evaluate their potentials. We also tried other kinds of SRs, such as triethanolamine (TEOA; Table 1), but none of them can outperform TEA. The reaction medium often has a dramatic effect on the performance of the H<sub>2</sub> evolution system.<sup>18</sup> The highest TON was obtained in a THF/water mixed solvent with a volume ratio of 8:2, which was used throughout the following H<sub>2</sub> evolution experiments. Unless otherwise noted, the concentrations of PS, WRC, and SR are 50 μM, 50 μM, and 0.6 M, respectively.

Figure 1 shows the time dependence of the TON values of our multicomponent systems. The TON data after 20 h of irradiation are presented in Table 2. In both cases of Rh<sub>2</sub>bpy<sub>2</sub>

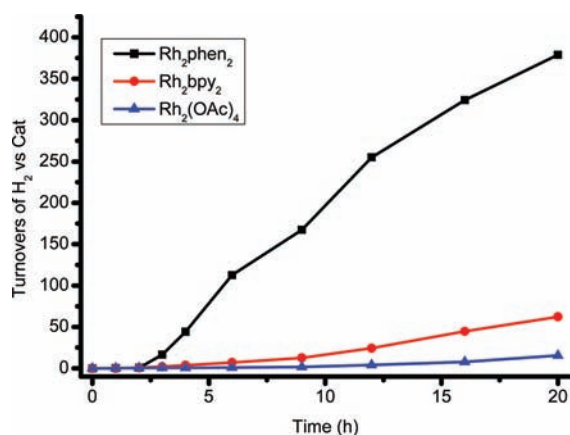


**Figure 1.** Time dependence of the photocatalytic H<sub>2</sub> production of the multicomponent systems containing 5.0 × 10<sup>-5</sup> M [Ir<sup>III</sup>(ppy)<sub>2</sub>(dtbbpy)]<sup>+</sup>, 0.6 M TEA, and a 5.0 × 10<sup>-5</sup> M Rh<sup>II</sup>-based catalyst in THF/water (8:2, v/v).

**Table 2. Turnover Number (TON) and Turnover Frequency (TOF) of the Multicomponent Systems Based on Different Dirhodium(II) Complexes and Selected Kinetic and Electrochemical Data**

complex	TON <sup>a</sup>	TOF (h <sup>-1</sup> ) <sup>a</sup>	quenching rate constants (M <sup>-1</sup> s <sup>-1</sup> )	E <sub>Rh<sup>II</sup>/Rh<sup>I</sup>/Rh<sup>III</sup></sub> (V, vs SCE) <sup>b</sup>	E <sub>Rh<sup>II</sup>/Rh<sup>I</sup>/Rh<sup>III</sup></sub> (V, vs SCE) <sup>b</sup>
Rh <sub>2</sub> (OAc) <sub>4</sub>	16	0.8	3.3 × 10 <sup>9</sup>	-0.85	
Rh <sub>2</sub> bpy <sub>2</sub>	62	3.1	3.6 × 10 <sup>9</sup>	-0.75	-1.46
Rh <sub>2</sub> phen <sub>2</sub>	379	19.0	2.6 × 10 <sup>9</sup>	-0.79	-1.52

<sup>a</sup>The data were obtained after 20 h of irradiation. <sup>b</sup>Peak potentials were determined by cyclic voltammetry in an anhydrous and deoxygenated DMSO solution.

and Rh<sub>2</sub>phen<sub>2</sub>, induction periods were observed. At the initial 3 h of irradiation, no appreciable H<sub>2</sub> was detected, and then the amount of H<sub>2</sub> increased gradually with irradiation. Rh<sub>2</sub>phen<sub>2</sub> proved to be the most active one of the examined catalysts, having a TON of up to 379 after 20 h of irradiation, while the TON values of Rh<sub>2</sub>bpy<sub>2</sub> and Rh<sub>2</sub>(OAc)<sub>4</sub> are only 62 and 16, respectively.

In Sakai's system, [Rh<sup>II</sup><sub>2</sub>(μ-O<sub>2</sub>CCH<sub>3</sub>)<sub>4</sub>(H<sub>2</sub>O)<sub>2</sub>] catalyzed the H<sub>2</sub> evolution more efficiently than Rh<sub>2</sub>(bpy)<sub>2</sub>. However, in our cases, Rh<sub>2</sub>(OAc)<sub>4</sub> is much inferior to Rh<sub>2</sub>bpy<sub>2</sub> or Rh<sub>2</sub>phen<sub>2</sub>, indicating the importance of the combination of PS and WRC. The reaction medium may also play a role.

What is more worth noting is the more than 6-fold enhancement in the catalytic activity from Rh<sub>2</sub>bpy<sub>2</sub> to Rh<sub>2</sub>phen<sub>2</sub>. Such a disparity in H<sub>2</sub> production between the two catalysts in otherwise identical conditions is remarkable and unexpected. Understanding the underlying mechanism is undoubtedly helpful for the further structure modification of such types of catalysts.

We carefully examined the concentration effect of Rh<sub>2</sub>phen<sub>2</sub> while maintaining PS and SR at 50 μM and 0.6 M, respectively (Figure 2). In the presence of 16.7 μM Rh<sub>2</sub>phen<sub>2</sub>, the H<sub>2</sub> production efficiency of the system reached the highest value; i.e., 4.4 mL of H<sub>2</sub> was obtained after 20 h of irradiation, corresponding to TON of 1182 or TOF of 59.1 h<sup>-1</sup>. A further increase of the concentration of Rh<sub>2</sub>phen<sub>2</sub> led to a decrease of the H<sub>2</sub> production rate, a phenomenon also observed for other Rh-based WRCs.<sup>18,24</sup>

The Rh<sub>2</sub>phen<sub>2</sub>-based multicomponent system exhibits good long-term durability in H<sub>2</sub> production. After 50 h of irradiation, the TON reached 772 for the case in which both PS and WRC are 50 μM, and the TOF (15.5 h<sup>-1</sup>) at 50 h experienced only a small decrease compared to that at 20 h (19.0 h<sup>-1</sup>); see Figure 3. At lower concentration of WRC (16.7 μM), the H<sub>2</sub> production rate maintained a higher value (Figures 2 and 3), and the TON reached 2622 after 50 h of irradiation. A reduced induction period (less than 1 h) was also observed in this case. In contrast, at a lower concentration of PS, the H<sub>2</sub> production rate decreased dramatically, although the durability of the system is still unaffected.

**Homogeneous or Heterogeneous Catalysis.** In any homogeneous system where reducing conditions exist, care must be taken to ensure that the catalytic activity originates from an actual molecular species and not a colloidal metal formed through catalyst decomposition.<sup>18</sup> A mercury poisoning test is a common approach to examining the contribution of colloidal metal. However, the strong interaction between mercury and Rh<sub>2</sub>bpy<sub>2</sub> or Rh<sub>2</sub>phen<sub>2</sub>, as shown in Figure S1 in

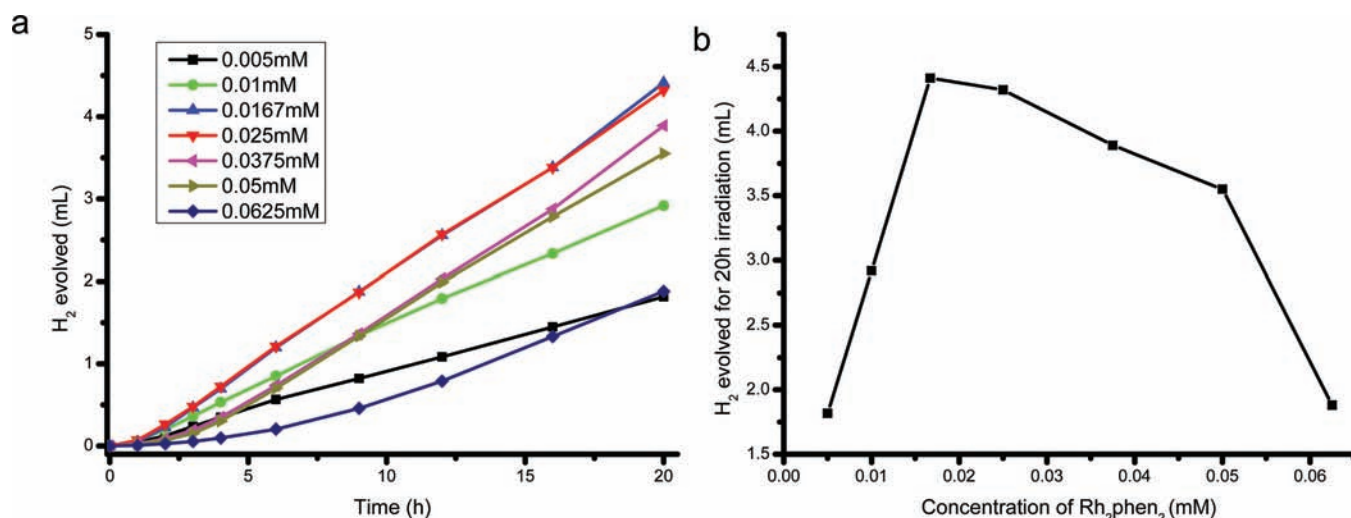


**Figure 2.** Dependence of the H<sub>2</sub> production efficiency on the concentration of Rh<sub>2</sub>phen<sub>2</sub>. The concentrations of [Ir<sup>III</sup>(ppy)<sub>2</sub>(dtbbpy)]<sup>+</sup> and TEA are 0.05 mM and 0.6 M, respectively.

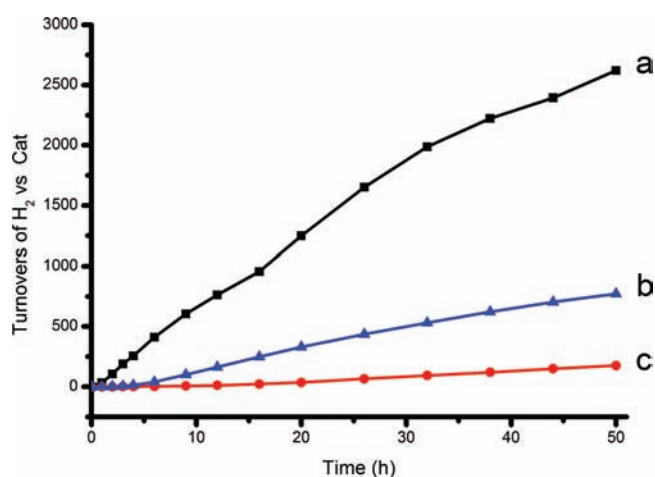


**Figure 3.** H<sub>2</sub> production of 10 mL of THF/water (8:2, v/v) solutions containing [Ir(ppy)<sub>2</sub>(dtbbpy)]<sup>+</sup>, Rh<sub>2</sub>phen<sub>2</sub>, and TEA (0.6 M) during 50 h of irradiation: (a) 50 μM [Ir(ppy)<sub>2</sub>(dtbbpy)]<sup>+</sup> and 16.7 μM Rh<sub>2</sub>phen<sub>2</sub>; (b) 50 μM [Ir(ppy)<sub>2</sub>(dtbbpy)]<sup>+</sup> and 50 μM Rh<sub>2</sub>phen<sub>2</sub>; (c) 16.7 μM [Ir(ppy)<sub>2</sub>(dtbbpy)]<sup>+</sup> and 50 μM Rh<sub>2</sub>phen<sub>2</sub>.

the Supporting Information, hindered the application of this method in our cases.

Figure 4 shows the absorption spectral changes of the multicomponent systems upon irradiation. After 3 h of irradiation, the spectrum no longer underwent discernible changes, in line with the induction periods observed in Figure 1, implying that both Rh<sub>2</sub>bpy<sub>2</sub> and Rh<sub>2</sub>phen<sub>2</sub> experienced some variations to acquire catalysis capability.

In the case of Rh<sub>2</sub>bpy<sub>2</sub>, irradiation led to a continued baseline increase of the absorption spectrum, suggesting the formation of colloidal particles. The irradiation of the Ir-based PS solution or TEA solution did not lead to any baseline increase in the absorption spectrum, confirming that the colloidal species stems from a rhodium catalyst rather than other components. The colloidal rhodium formed during the induction period may at least partly account for the catalytic activity of the Rh<sub>2</sub>bpy<sub>2</sub>-based system that presented after the induction period.

In contrast, after the first 0.5 h of irradiation, the absorption baseline of the Rh<sub>2</sub>phen<sub>2</sub>-based system remained unchanged. At this moment, the catalytic activity of the system was still very low. Thus, the much higher catalytic activity of Rh<sub>2</sub>phen<sub>2</sub> presented after 3 h of irradiation does not likely originate

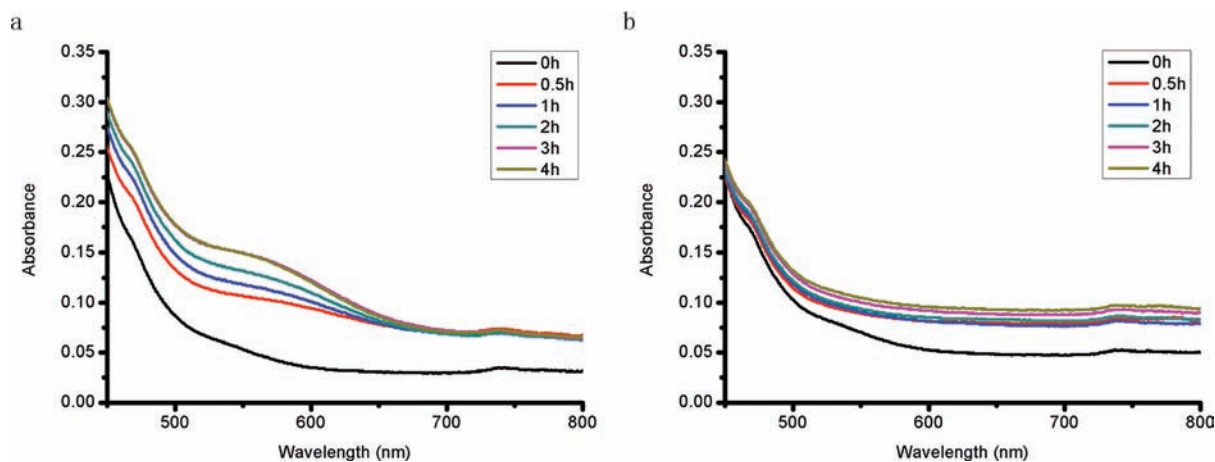


**Figure 4.** Absorption spectral changes of the multicomponent systems based on Rh<sub>2</sub>phen<sub>2</sub> (a) and Rh<sub>2</sub>bpy<sub>2</sub> (b) during photocatalytic H<sub>2</sub> production. 0.05 mM [Ir(ppy)<sub>2</sub>(dtbbpy)]<sup>+</sup>, 0.6 M TEA, and 0.05 mM dirhodium(II) catalyst in 10 mL of THF/water (8:2, v/v).

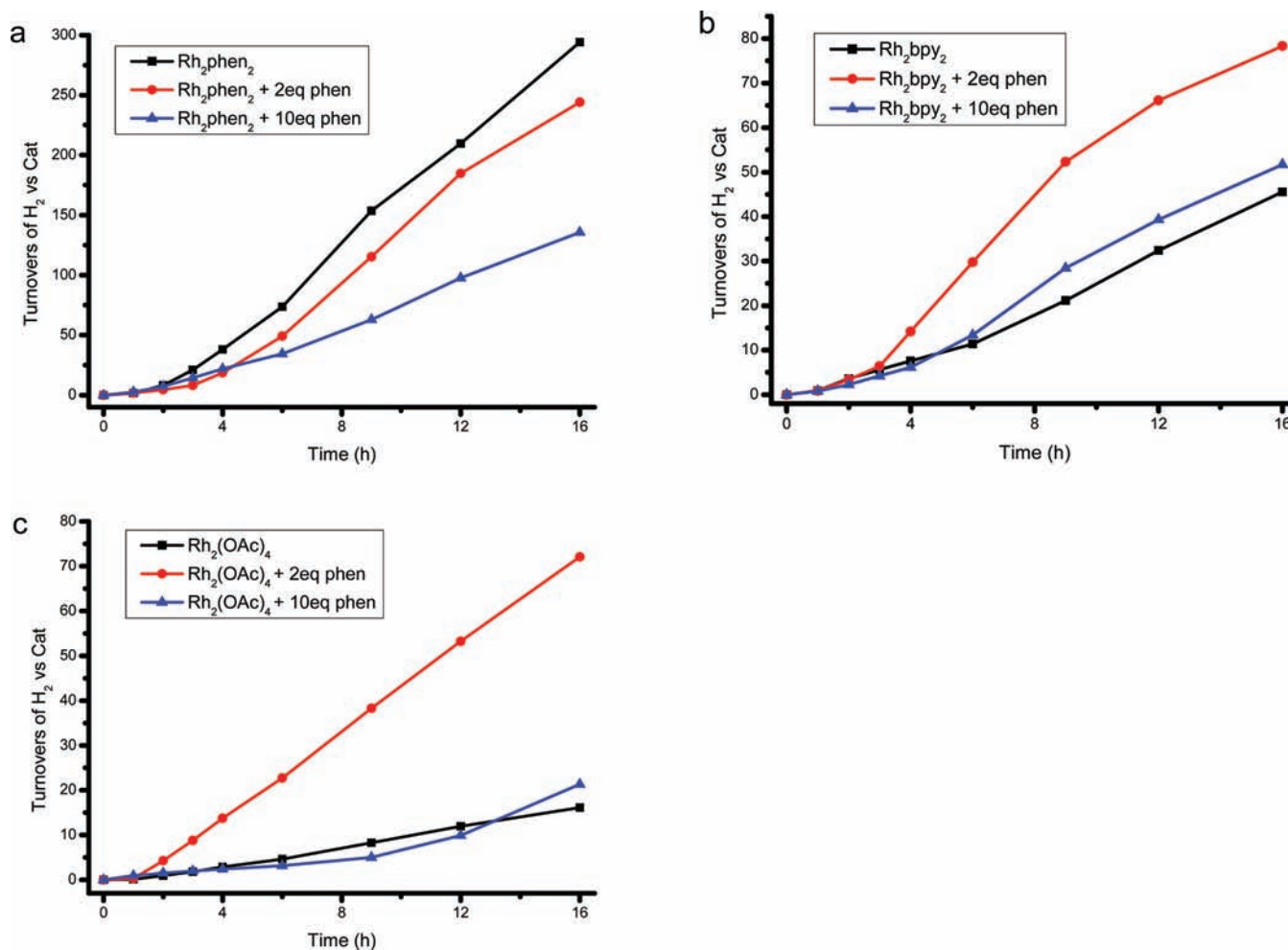


**Figure 5.** Effects of the free phen ligand on the photocatalytic H<sub>2</sub> production of the multicomponent systems based on Rh<sub>2</sub>phen<sub>2</sub> (a), Rh<sub>2</sub>bpy<sub>2</sub> (b), and Rh<sub>2</sub>(OAc)<sub>4</sub> (c). The concentrations of [Ir(ppy)<sub>2</sub>(dtbbpy)]<sup>+</sup>, TEA, and the catalyst are 0.05 mM, 0.6 M, and 0.05 mM, respectively. The concentrations of the added phen are respectively 2 and 10 equiv with respect to the catalyst.

from the colloidal rhodium as in the case of Rh<sub>2</sub>bpy<sub>2</sub>. Noticeably, the irradiation, particularly in the period of 0.5–3 h, gave rise to the appearance of a new absorption band within 500–600 nm, having the absorption maximum at around 575 nm. After 3 h of irradiation, this new 575-nm-absorbing species remained unchanged, while the system began to produce H<sub>2</sub> at a constant rate. Although the structure of this 575-nm intermediate is unknown at present, one may expect that it is this species that accounts for the significant difference in the catalytic activities between Rh<sub>2</sub>bpy<sub>2</sub> and Rh<sub>2</sub>phen<sub>2</sub>.

Another possibility should be taken into consideration also; i.e., a specific interaction exists between the colloidal rhodium and the phen ligands, which gives rise to this specific absorption at 575 nm. We examined the effects of the phen ligand on the catalytic activities of Rh<sub>2</sub>phen<sub>2</sub>, Rh<sub>2</sub>bpy<sub>2</sub>, and Rh<sub>2</sub>(OAc)<sub>4</sub> systems. As shown in Figure 5a, the presence of phen at either 2 equiv (0.1 mM) or 10 equiv (0.5 mM) decreased the catalytic activity of Rh<sub>2</sub>phen<sub>2</sub> remarkably. Figure 6a shows the corresponding absorption changes during the irradiation. The addition of phen did not restrict the baseline increase, i.e., the colloidal rhodium formation. If the 575-nm intermediate originates from the interaction between the colloidal rhodium and phen, the addition of phen will facilitate such an interaction and increase the catalytic activity of the system. However, the absorbance at 575 nm did not increase and the catalytic activity

of the system decreased, ruling out the origin of the 575-nm intermediate from such an interaction. Instead, a new absorption band centered at 390 nm was observed, suggesting the formation of a new species, which may impair the catalytic activity of the 575-nm intermediate.

Interestingly, the addition of phen enhanced the catalytic activities of Rh<sub>2</sub>bpy<sub>2</sub> and Rh<sub>2</sub>(OAc)<sub>4</sub>, particularly at 2 equiv, as shown in Figure 5b,c. The insets of Figure 6b,c show the emergence of the 575-nm absorption band. The ligand substitution between bpy and phen or between OAc and phen may contribute to the formation of the 575-nm intermediate, which, in turn, improves the catalytic activity of the system. However, the formation of the 575-nm intermediate is obviously less efficient than the case of Rh<sub>2</sub>phen<sub>2</sub>. Moreover, other species that have strong absorbance around 400 nm appeared during irradiation, which might interfere with the H<sub>2</sub> production process. As a result, the catalytic activities of the two systems are far less efficient than that of Rh<sub>2</sub>phen<sub>2</sub>. In both cases, irradiation led to an absorption baseline increase, in accordance with the formation of the colloidal rhodium. If the 575-nm intermediate results from the interaction of the colloidal rhodium and phen, the addition of 10 equiv of phen will improve the catalytic activity more efficiently than the case of 2 equiv. The experimental observation (Figure 5) precludes such a further possibility.

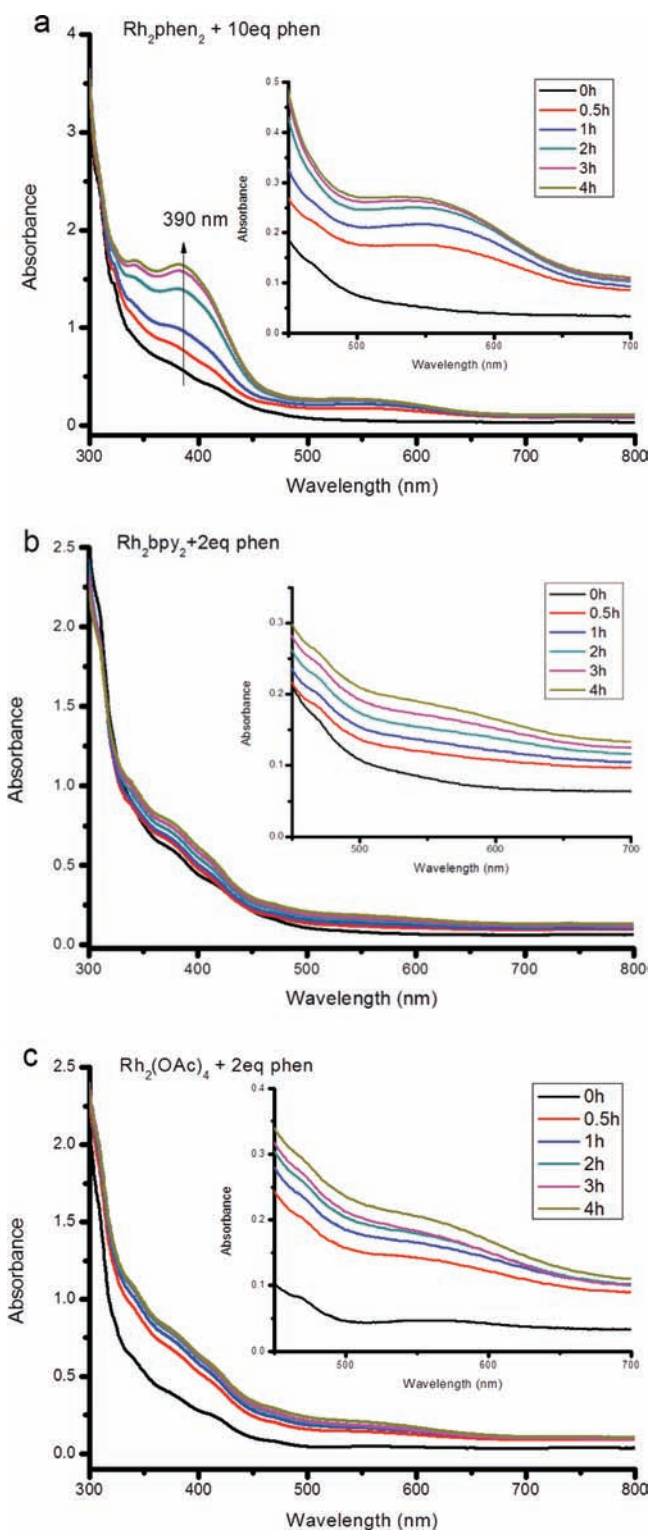


**Figure 6.** Absorption spectral changes of the multicomponent systems based on Rh<sub>2</sub>phen<sub>2</sub> (a), Rh<sub>2</sub>bpy<sub>2</sub> (b), and Rh<sub>2</sub>(OAc)<sub>4</sub> (c) during photocatalytic H<sub>2</sub> production in the presence of the free phen ligand. 0.05 mM [Ir(ppy)<sub>2</sub>(dtbppy)]<sup>+</sup>, 0.6 M TEA, and 0.05 mM dirhodium(II) catalyst in 10 mL of THF/water (8:2, v/v). The added phen is either 2 or 10 equiv with respect to the catalyst.

**Electrocatalytic H<sub>2</sub> Production.** The studies on the electrocatalytic activities of the examined rhodium catalysts may shed light on their photocatalytic activities. Figure 7 shows the cyclic voltammograms of Rh<sub>2</sub>phen<sub>2</sub> and Rh<sub>2</sub>bpy<sub>2</sub> in DMSO.

For Rh<sub>2</sub>phen<sub>2</sub>, two redox couples are observed at  $-0.79$  and  $-1.52$  V vs SCE, which are assignable to Rh<sup>II</sup>Rh<sup>II</sup>/Rh<sup>II</sup>Rh<sup>I</sup> and Rh<sup>II</sup>Rh<sup>I</sup>/Rh<sup>I</sup>Rh<sup>I</sup> processes, respectively. The addition of acetic acid triggers the appearance of a catalytic reduction wave near the redox potential of the Rh<sup>II</sup>Rh<sup>I</sup>/Rh<sup>I</sup>Rh<sup>I</sup> couple, suggesting that the Rh<sup>I</sup>Rh<sup>I</sup> species is the actual active species in proton reduction. Similarly, the Rh<sup>II</sup>Rh<sup>II</sup>/Rh<sup>II</sup>Rh<sup>I</sup> and Rh<sup>II</sup>Rh<sup>I</sup>/Rh<sup>I</sup>Rh<sup>I</sup> potentials of Rh<sub>2</sub>bpy<sub>2</sub> locate at  $-0.75$  and  $-1.46$  V vs SCE, respectively. Upon the addition of acetic acid, reduction current enhancement occurred also at the second reduction potential, implying that the proton reduction active species is also Rh<sup>I</sup>Rh<sup>I</sup> for Rh<sub>2</sub>bpy<sub>2</sub>.

These results demonstrate that both Rh<sub>2</sub>bpy<sub>2</sub> and Rh<sub>2</sub>phen<sub>2</sub> should accept two electrons prior to participating in the proton reduction in the multicomponent photocatalytic H<sub>2</sub> production systems. As shown below, the initial photoreaction in our photocatalytic systems is the reduction of the excited Ir-based PS by TEA. The redox potential of [Ir]/[Ir]<sup>-</sup> couples was measured to be  $-1.45$  V vs SCE. It is then clear that the collection of the second electron from the reduced PS is not a downhill process, although the collection of the first electron is thermodynamically favorable. As a result, Rh<sub>2</sub>bpy<sub>2</sub> and Rh<sub>2</sub>phen<sub>2</sub> need to transform to a new species that can accept two electrons from the reduced PS to catalyze the proton reduction.

The inhibitory effect of MV<sup>2+</sup> (with a reduction potential at  $-0.68$  V vs SCE<sup>30</sup>) on the catalytic activities of Rh<sub>2</sub>bpy<sub>2</sub> and Rh<sub>2</sub>phen<sub>2</sub> might also be due to the more negative reduction potentials of the complexes or the 575-nm intermediate (in particular, the second reduction potential), which makes MV<sup>2+</sup> serve as an electron trap rather than a ER in the multicomponent system. The low reduction potentials of Rh<sub>2</sub>bpy<sub>2</sub> and Rh<sub>2</sub>phen<sub>2</sub> would limit the choice of a PS and lower the driving force for electron transfer from PS to WRC. Accordingly, our future effort will be on the design and synthesis of dirhodium complexes with less negative reduction potentials. On the other hand, the omission of an ER such as MV<sup>2+</sup> may simplify the system and mitigate the energy loss occurring in multistep electron-transfer processes, thus enhancing the electron-transfer efficiency.

#### Luminescence Quenching and Transient Absorption.

To realize H<sub>2</sub> production, a precondition is the photoinduced electron transfer between PS, WRC, and SR (no ER in our cases). Thus, the luminescence quenching of the Ir-based PS by Rh<sub>2</sub>phen<sub>2</sub>, Rh<sub>2</sub>bpy<sub>2</sub>, and TEA was investigated.

As shown in Figure S2 in the Supporting Information,  $\tau_0/\tau$  was plotted as a function of the quencher concentration, where  $\tau_0$  and  $\tau$  are the luminescence lifetimes of PS in the absence and presence of a quencher, respectively. Fitting the data by way of the Stern–Volmer equation (eq 1) allows for determination of the dynamic quenching rate constants  $3.6 \times 10^9$  M<sup>-1</sup> s<sup>-1</sup> for Rh<sub>2</sub>bpy<sub>2</sub>,  $2.6 \times 10^9$  M<sup>-1</sup> s<sup>-1</sup> for Rh<sub>2</sub>phen<sub>2</sub>, and  $2.6 \times 10^7$  M<sup>-1</sup> s<sup>-1</sup> for TEA (Table 2). The luminescence quenching is mainly due to the single electron transfer from the excited PS to the Rh-based catalyst. As mentioned above, to achieve the catalytic activity, the Rh-based catalyst should accept two electrons. Consequently, there is no correlation between the quenching rate constants and the H<sub>2</sub> evolution efficiencies. For example, although Rh<sub>2</sub>bpy<sub>2</sub> quenches the luminescence of the Ir-based PS more efficiently than Rh<sub>2</sub>phen<sub>2</sub>, its catalytic activity is much lower than that of Rh<sub>2</sub>phen<sub>2</sub>.

$$\tau_0/\tau = 1 + k_q\tau_0[Q] \quad (1)$$

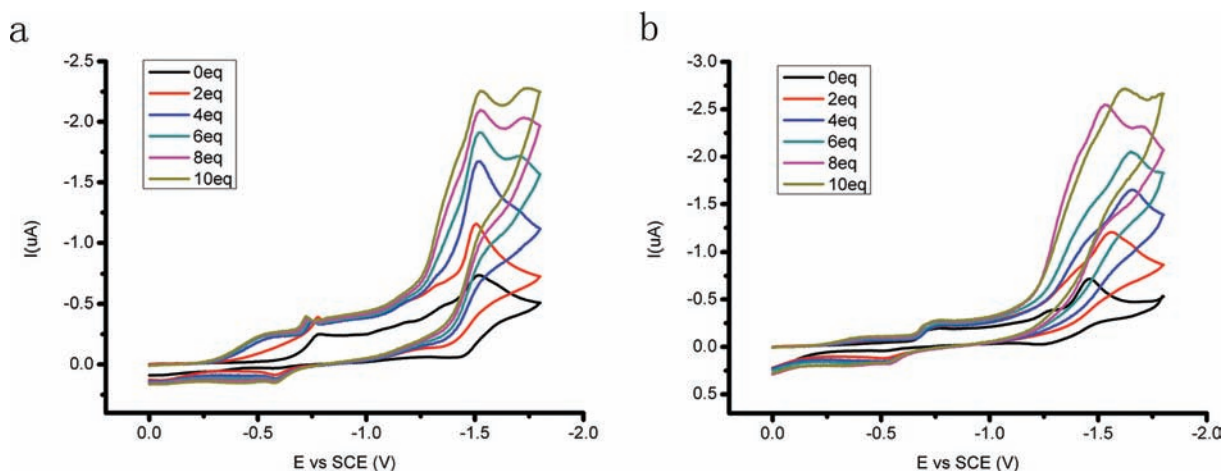


**Figure 7.** Electrochemical properties of  $\text{Rh}_2\text{phen}_2$  (a) and  $\text{Rh}_2\text{bpy}_2$  (b) in DMSO in the presence of various concentrations of acetic acid.

Although the quenching rate constants of the catalysts are 2 orders of magnitude larger than that of TEA, reductive quenching (i.e., electron transfer from TEA to the excited PS) dominates in our system because of the much larger concentration of TEA (0.6 M) than that of the catalysts ( $5 \times 10^{-5}$  M). Therefore, in our multicomponent systems, the main electron donor is the reduced PS rather than the excited PS for the catalysts. Transient absorption spectra are in line with this conclusion (Figure 8). The transient absorption spectrum of Ir-

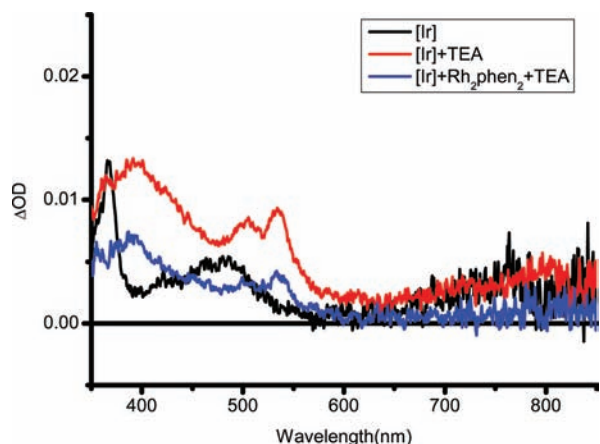


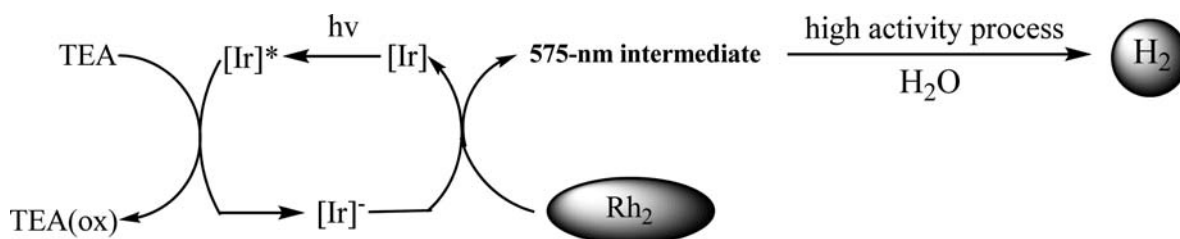
**Figure 8.** Transient absorption spectra of the solutions containing Ir-based PS only (a), Ir-based PS and TEA (b), and Ir-based PS, TEA, and  $\text{Rh}_2\text{phen}_2$  (c), recorded after a 200 ns delay of the laser irradiation at 420 nm.

based PS exhibits two bands centered at 365 and 480 nm, respectively, attributable to the excited PS in the triplet multiplicity.<sup>29</sup> The addition of TEA leads to remarkable spectral changes, showing three bands centered at 393, 504, and 536 nm, respectively, assignable to the reduced PS. A further addition of the Rh-based catalyst does not alter the spectrum profile but decreases the spectrum intensity, in accordance with electron transfer from the reduced PS to the catalyst. We also measured the transient absorption spectra of the multicomponent systems that had been irradiated for 20 h. The obtained spectra are similar to that of the mixture of Ir-based PS and TEA (Figure S3 in the Supporting Information), vindicating further that the initial and predominant photo-reaction is the reductive quenching of the excited PS by TEA.

**Photostability.** In order to identify the chemical nature of the 575-nm intermediate, we examined the photoinduced products of  $\text{Rh}_2\text{bpy}_2$  and  $\text{Rh}_2\text{phen}_2$  in argon-saturated THF/water (8:2, v/v) in the absence of Ir-based PS and TEA. As shown in Figure S4 in the Supporting Information, both  $\text{Rh}_2\text{bpy}_2$  and  $\text{Rh}_2\text{phen}_2$  are not stable upon irradiation. However, no 575-nm band as well as baseline increase was found, suggesting neither the 575-nm intermediate nor the colloidal rhodium formed. After irradiation for 3 or 9 h, Ir-based PS and TEA were added to construct the multicomponent systems; however, no  $\text{H}_2$  evolution was detected. These results indicate that the 575-nm intermediate is the photoproduct of  $\text{Rh}_2\text{phen}_2$  in the presence of PS and TEA, where the photoinduced electron transfer between them may play a key role.

**Overall Mechanism of  $\text{H}_2$  Evolution.** A mechanism for the photocatalytic  $\text{H}_2$  production of the multicomponent system based on  $\text{Rh}_2\text{phen}_2$  may be put forth as in Scheme 2.

**Scheme 2.** Proposed Photocatalytic  $\text{H}_2$  Production Mechanism for the Multicomponent System Containing an Ir-Based PS, a TEA-Based SR, and a  $\text{Rh}_2\text{phen}_2$ -Based Catalyst



Upon irradiation, the excited PS ( $[\text{Ir}]^*$ , most likely in the triplet excited state due to the ultrafast intersystem crossing of the Ir-based complexes) is reduced to  $[\text{Ir}]^-$  by TEA. Then, electron transfer from  $[\text{Ir}]^-$  to  $\text{Rh}_2\text{phen}_2$  favors the latter to experience some structure variation to form the 575-nm intermediate, by which the  $\text{H}_2$  evolution is catalyzed. For  $\text{Rh}_2\text{bpy}_2$ , no active species similar to the 575-nm intermediate forms during irradiation, and the low  $\text{H}_2$  evolution efficiency partly results from the colloidal rhodium.

The observed disparity in the photocatalytic activity between  $\text{Rh}_2\text{bpy}_2$  and  $\text{Rh}_2\text{phen}_2$  must come from the different diimine ligands used. Before identification of the nature of the 575-nm intermediate, any convincing explanation is difficult to reach. We believe further exploration of such types of dirhodium(II) complexes bearing other kinds of diimine ligands will be helpful in understanding the underlying mechanism and the development of more efficient photocatalytic  $\text{H}_2$  production systems.

## CONCLUSION

In summary, the  $\text{H}_2$  evolution catalysis activities of two dirhodium(II) complexes,  $\text{Rh}_2\text{bpy}_2$  and  $\text{Rh}_2\text{phen}_2$ , were studied in a multicomponent system, using  $[\text{Ir}^{\text{III}}(\text{ppy})_2(\text{dtbbpy})]^+$  as a PS and TEA as a SR. Both  $\text{Rh}_2^{\text{II}}$ -based catalysts are greatly superior to the  $\text{Rh}_2(\mu\text{-O}_2\text{CCH}_3)_4$  model complex. More importantly, there is more than a 6-fold increase in the photocatalytic activity from  $\text{Rh}_2\text{bpy}_2$  to  $\text{Rh}_2\text{phen}_2$  just using phen in place of bpy. The results clearly highlight the importance of N-based chelate ligands for the dirhodium(II) compounds. Further work is underway to develop new  $\text{Rh}_2^{\text{II}}$ -based catalysts for better understanding the mechanism and higher photocatalytic  $\text{H}_2$  production efficiency.

## ASSOCIATED CONTENT

### Supporting Information

Absorption spectral changes, Stern–Volmer quenching, transient absorption spectra, and time dependence of the absorption spectral changes. This material is available free of charge via the Internet at <http://pubs.acs.org>.

## AUTHOR INFORMATION

### Corresponding Author

\*Tel.: +86-10-82543592. Fax: +86-10-62564049. E-mail: [xswang@mail.ipc.ac.cn](mailto:xswang@mail.ipc.ac.cn) (X.W.), [yuanjunhou@yahoo.com](mailto:yuanjunhou@yahoo.com) (Y.H.).

### Notes

The authors declare no competing financial interest.

## ACKNOWLEDGMENTS

This work was financially supported by the NSFC (Grant Nos. 21101163 and 21172228) and CAS (Grant No. KG CX2YW-389).

## REFERENCES

- (1) Esswein, A. J.; Nocera, D. G. *Chem. Rev.* **2007**, *107*, 4022.
- (2) Tinker, L. L.; McDaniel, N. D.; Bernhard, S. *J. Mater. Chem.* **2009**, *19*, 3328.
- (3) Armaroli, N.; Balzani, V. *Angew. Chem., Int. Ed.* **2007**, *46*, 52.
- (4) Concepcion, J. J.; Jurss, J. W.; Templeton, J. L.; Meyer, T. J. *J. Am. Chem. Soc.* **2008**, *130*, 16462.
- (5) (a) Xu, Y.; Duan, L.; Tong, L.; Akermark, B.; Sun, L. *Chem. Commun.* **2010**, *46*, 6506. (b) Xu, Y.; Fischer, A.; Duan, L.; Tong, L.; Gabrielsson, E.; Akermark, B.; Sun, L. *Angew. Chem., Int. Ed.* **2010**, *49*, 8934.

- (6) Ozawa, H.; Sakai, K. *Chem. Commun.* **2011**, *47*, 2227.
- (7) (a) Du, P.; Knowles, K.; Eisenberg, R. *J. Am. Chem. Soc.* **2008**, *130*, 12576. (b) Du, P.; Schneider, J.; Luo, G.; Brennessel, W.; Eisenberg, R. *Inorg. Chem.* **2009**, *48*, 4952.
- (8) He, L.; Luo, C.; Hou, Y.; Li, C.; Zhou, Q.; Sun, Y.; Wang, W.; Zhang, B.; Wang, X. *Int. J. Hydrogen Energy* **2011**, *36*, 10593.
- (9) (a) Lehn, J.-M.; Sauvage, J.-P. *Nouv. J. Chim.* **1977**, *1*, 449. (b) Kirch, M.; Lehn, J.-M.; Sauvage, J.-P. *Helv. Chim. Acta* **1979**, *62*, 1345.
- (10) (a) Brown, G. M.; Chan, S.-F.; Creutz, C.; Schwarz, H. A.; Sutin, N. *J. Am. Chem. Soc.* **1979**, *101*, 7638. (b) Chan, S.-F.; Chou, M.; Creutz, C.; Matsubara, T.; Sutin, N. *J. Am. Chem. Soc.* **1981**, *103*, 369.
- (11) (a) Goldsmith, J.; Hudson, W.; Lowry, M.; Anderson, T.; Bernhard, S. *J. Am. Chem. Soc.* **2005**, *127*, 7502. (b) DiSalle, B. F.; Bernhard, S. *J. Am. Chem. Soc.* **2011**, *133*, 11819.
- (12) (a) Du, P.; Eisenberg, R. *Energy Environ. Sci.* **2012**, *5*, 6012. (b) Lazarides, T.; McCormick, T.; Du, P.; Luo, G.; Lindley, B.; Eisenberg, R. *J. Am. Chem. Soc.* **2009**, *131*, 9192. (c) McCormick, T.; Calitree, B.; Orchard, A.; Kraut, N.; Bright, F.; Detty, M.; Eisenberg, R. *J. Am. Chem. Soc.* **2010**, *132*, 15480.
- (13) (a) Gartner, F.; Sundararaju, B.; Surkus, A. E.; Boddien, A.; Loges, B.; Junge, H.; Dixneuf, P. H.; Beller, M. *Angew. Chem., Int. Ed.* **2009**, *48*, 9962. (b) Wang, F.; Wang, W.-G.; Wang, X.-J.; Wang, H.-Y.; Tung, C.-H.; Wu, L.-Z. *Angew. Chem., Int. Ed.* **2011**, *50*, 3193.
- (14) (a) McLaughlin, M. P.; McCormick, T. M.; Eisenberg, R.; Holland, P. L. *Chem. Commun.* **2011**, *47*, 7989. (b) Han, Z.; McNamara, W. R.; Eum, M.-S.; Holland, P. L.; Eisenberg, R. *Angew. Chem., Int. Ed.* **2012**, *51*, 1667.
- (15) (a) Probst, B.; Kolano, C.; Hamm, P.; Alberto, R. *Inorg. Chem.* **2009**, *48*, 1836. (b) Probst, B.; Rodenberg, A.; Guttentag, M.; Hamm, P.; Alberto, R. *Inorg. Chem.* **2010**, *49*, 6453.
- (16) (a) Rau, S.; Schafer, B.; Gleich, D.; Anders, E.; Rudolph, M.; Friedrich, M.; Gorls, H.; Henry, W.; Vos, J. G. *Angew. Chem., Int. Ed.* **2006**, *45*, 6215. (b) Wang, X.; Goeb, S.; Ji, Z.; Pogulaichenko, N.; Castellano, F. *Inorg. Chem.* **2011**, *50*, 705.
- (17) (a) Artero, V.; Chavarot-Kerlidou, M.; Fontecave, M. *Angew. Chem., Int. Ed.* **2011**, *50*, 7238. (b) Fihri, A.; Artero, V.; Pereira, A.; Fontecave, M. *Dalton Trans.* **2008**, 5567.
- (18) Cline, E.; Adamson, S.; Bernhard, S. *Inorg. Chem.* **2008**, *47*, 10378.
- (19) Sutin, N.; Creutz, C.; Fujita, E. *Comments Inorg. Chem.* **1997**, *1967*.
- (20) (a) Elvington, M.; Brown, J.; Arachchige, S. M.; Brewer, K. J. *J. Am. Chem. Soc.* **2007**, *129*, 10644. (b) Arachchige, S.; Brown, J.; Chang, E.; Jain, A.; Zigler, D.; Rangan, K.; Brewer, K. *Inorg. Chem.* **2009**, *48*, 1989.
- (21) (a) Wang, J.; White, T. A.; Arachchige, S. M.; Brewer, K. J. *Chem. Commun.* **2011**, *47*, 4451. (b) White, T. A.; Whitaker, B. N.; Brewer, K. J. *J. Am. Chem. Soc.* **2011**, *133*, 15332. (c) White, T. A.; Higgins, S. L. H.; Arachchige, S. M.; Brewer, K. J. *Angew. Chem., Int. Ed.* **2011**, *50*, 12209.
- (22) Mann, K. R.; Lewis, N. S.; Miskowski, V. M.; Erwin, D. K.; Hammond, G. S.; Gray, H. B. *J. Am. Chem. Soc.* **1977**, *99*, 5525.
- (23) (a) Heyduk, A. F.; Nocera, D. G. *Science* **2001**, *293*, 1639. (b) Esswein, A. J.; Veige, A. S.; Nocera, D. G. *J. Am. Chem. Soc.* **2005**, *127*, 16641. (c) Rosenthal, J.; Bachman, J.; Dempsey, J. L.; Esswein, A. J.; Gray, T. G.; Hodgkiss, J. M.; Manke, D. R.; Luckett, T. D.; Pistorio, B. J.; Veige, A. S.; Nocera, D. G. *Coord. Chem. Rev.* **2005**, *249*, 1316.
- (24) Tanaka, S.; Masaoka, S.; Yamauchi, K.; Annaka, M.; Sakai, K. *Dalton Trans.* **2010**, *39*, 11218.
- (25) Lowry, M. S.; Hudson, W. R.; Pascal, R. A.; Bernhard, S. *J. Am. Chem. Soc.* **2004**, *126*, 14129.
- (26) Rempel, G. A.; Legzdins, P.; Smith, H.; Wilkinson, G. *Inorg. Synth.* **1972**, *13*, 90.
- (27) Crawford, C. A.; Matonic, J. H.; Huffman, J. C.; Foltling, K.; Dunbar, K. R.; Christou, G. *Inorg. Chem.* **1997**, *36*, 2361.
- (28) Angeles-Boza, A. M.; Chifotides, H. T.; Aguirre, J. D.; Chouai, A.; Fu, P. K. L.; Dunbar, K. R.; Turro, C. J. *Med. Chem.* **2006**, *49*, 6841.

- (29) Felici, M.; Contreras-Carballada, P.; Vida, Y.; Smits, J. M. M.; Nolte, R. J. M.; De Cola, L.; Williams, R. M.; Feiters, M. C. *Chem.—Eur. J.* **2009**, *15*, 13124.
- (30) Kaifer, A. E.; Bard, A. J. *J. Phys. Chem.* **1985**, *89*, 4876.